Science of the Total Environment 948 (2024) 174927

Contents lists available at ScienceDirect

Science of the Total Environment

journal homepage: www.elsevier.com/locate/scitotenv

# Prioritising urban heat island mitigation interventions: Mapping a heat risk index

Esraa Elmarakby[a,*], Hisham Elkadi[b]

[a] The University of Salford, School of Science, Engineering, and Environment, United Kingdom; Ain Shams University, Faculty of Engineering, Egypt
[b] The University of Salford, School of Science, Engineering, and Environment, United Kingdom

## HIGHLIGHTS

- Approximately one-third of Manchester experiences the UHI effect, with hot-spots concentrated closer to the city centre.
- The development of the Heat Risk Index (HRI) can guide the implementation of targeted interventions to mitigate UHI effects in metropolitan areas.
- HRI identified districts in Manchester with intensified UHI, correlating with high population density, lack of green cover, and higher LST.
- Applying the Heat Risk Index (HRI) at a micro-scale would enhance accuracy in analysis and enable the implementation of more targeted strategies.

## GRAPHICAL ABSTRACT

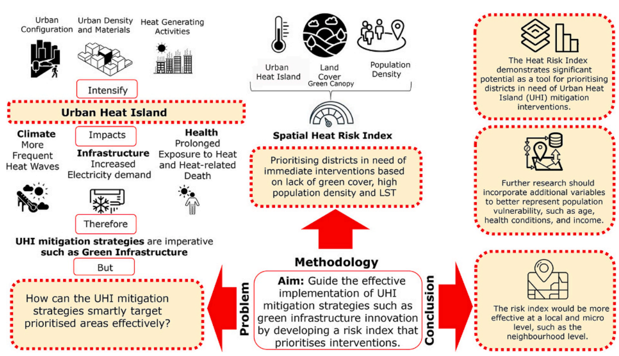


## ARTICLE INFO

Editor: Pavlos Kassomenos

*Keywords:*
Climate change
Urban Heat Islands (UHI)
Land surface temperature (LST) heat waves
Land cover
Heat risk index (HEI)
Remote sensing
Green infrastructure

## ABSTRACT

The global climate is under threat from increasing extreme heat, evidenced by rising temperatures and a surge in hot days. Heat waves are intensifying worldwide, impacting cities and residents, as demonstrated by the record-breaking heat experienced in the UK in 2022, which resulted in over 4500 deaths. Urban heat islands (UHIs) exacerbate these heat waves, making city residents more vulnerable to heat-related deaths. UHIs occur when temperatures in urban areas exceed those in surrounding rural areas due to the heat-absorbing properties of urban structures. Implementing mitigation strategies, such as green infrastructure, is crucial for enhancing urban resilience and reducing vulnerability to UHIs.

Effectively addressing UHIs requires a systematic approach, including developing risk maps to prioritise areas for UHI mitigation strategies. Using remote sensing, GIS, and SPSS correlational analysis, the research aims to develop and assess a Heat Risk Index (HRI). This index integrates UHI spatial intensity, current green cover, and population density at the district level to develop the risk index. This study stands out for its novel approach to developing the HRI, focusing on the localised impact of the UHI in Manchester City, identifying high-risk heat-vulnerable districts, and prioritising implementing effective UHI mitigation strategies.

The findings highlight the importance of this approach, revealing that approximately 30 % of Manchester City is affected by UHI effects, with areas near the city centre, characterised by higher population density and reduced green cover, being particularly vulnerable. Furthermore, the study suggests that applying HRIs at a more localised level, such as the neighbourhood level rather than the district level, would provide more relevant and

* Corresponding author.
*E-mail addresses:* e.a.h.i.elmarakby@edu.salford.ac.uk (E. Elmarakby), H.Elkadi@salford.ac.uk (H. Elkadi).

https://doi.org/10.1016/j.scitotenv.2024.174927
Received 6 May 2024; Received in revised form 28 June 2024; Accepted 19 July 2024
Available online 20 July 2024

targeted insights for mitigating UHI. A more localised index would offer tailored insights into the unique conditions of each neighbourhood within the districts, enabling more effective mitigation strategies. The HRI developed in this paper serves as a test for a more nuanced and comprehensive index, considering additional variables related to population vulnerability and city urban structure.

## 1. Literature review

Climate change refers to long-term alterations in temperature, precipitation patterns, and other atmospheric conditions on Earth (Calabrese et al., 2024; Mirza, 2003; Stott, 2016). These changes in the weather pattern are attributed to human activities, particularly the burning of fossil fuels, deforestation, and industrial processes that release greenhouse gases into the atmosphere (Stott, 2016). One of the most significant consequences of climate change is the increase in the frequency and intensity of extreme weather events (Calabrese et al., 2024; Mirza, 2003).

Heatwaves are among the most noticeable impacts of climate change (Marx et al., 2021). Extreme heat events encompass meteorological conditions that significantly deviate from the typical severity, frequency, or expectations within a local climate (Hopke, 2020; Marx et al., 2021). In the era of climate change, the prevalence of extreme heat translates to increased occurrences of heatwaves, characterised by prolonged periods of exceptionally high temperatures (Hopke, 2020). The impacts of these intense heat events can be profound and often result in adverse consequences for ecosystems, human health, and various societal sectors (Calabrese et al., 2024; Hopke, 2020; Mirza, 2003).

According to the UK Royal Meteorological Society (RMetS) report, 2022 emerged as the warmest year in the UK since 1884, surpassing the 1991–2020 average by 0.9 °C (Kendon et al., 2023; Met Office, 2023b). Notably, it marked the first time a UK annual mean temperature exceeded 10 °C (Met Office, 2023b). In 2022, the country witnessed an unprecedented heatwave, with temperatures hitting 40 °C for the first time, significantly exceeding previous records (Kendon et al., 2023).

Furthermore, all four seasons that year—winter, spring, summer, and autumn— were ranked among the top 10 warmest in the UK series since 1884 (Kendon et al., 2023; Met Office, 2023b).

The RMetS report underscored that the 21st century has seen all top-10 warmest years for the UK since 1884. The recent decade (2013−2022) averaged 0.3 °C higher than the 1991–2012 average and 1.1 °C warmer than the 1961–1990 period. Significantly, this decade represents the warmest 10-year period (Hanlon et al., 2021; Met Office, 2023a).

In terms of duration, The UK's climate extremes report (2023a) indicated a recent pattern of elevated maximum temperatures and extended warm spells (Met Office, 2023a). The average duration of these warm spells has more than doubled, increasing from 5.3 days in 1961–90 to over 13 days during 2008–2017. This trend is particularly pronounced in Southeast England, where warm spells have surged from around six days in 1961–90 to an average of over eighteen days per year from 2008 to 2017 (Met Office, 2023a).

In addition, the UK Climate Projections (UKCP) (2024), utilising high carbon emission scenarios, forecasted a considerable rise in outdoor temperatures across the UK. This projection indicated a potential increase of up to 5.4 degrees Celsius by 2070. These projections underscore the enduring repercussions of human-induced climate change, underscoring the critical necessity for implementing prompt and effective climate change mitigation and adaptation measures.

All these statistics unmistakably indicate that climate change is indeed happening, and no country is immune to its effects. Therefore, cities must remain vigilant, systematic, and strategic in their approach to addressing it.

### 1.1. Climate change and extreme heat waves

Extended periods of extreme heat, particularly during the summer, can have profound implications for public health, notably contributing to a heightened mortality rate (Dong et al., 2020). The intensified temperatures associated with prolonged hot spells amplify the risks of various health conditions, increasing morbidity and mortality (Arsad et al., 2022).

The most direct health impacts of extreme heat include dehydration and heat exhaustion, both of which can strain the body's ability to regulate temperature (Arsad et al., 2022). Vulnerable populations, such as older people, young children, and individuals with pre-existing health conditions, are particularly susceptible to heat-related illnesses (Dong et al., 2020; Maragno et al., 2020). Prolonged exposure to high temperatures may exacerbate chronic conditions, leading to severe health complications and, in some cases, fatalities (Dong et al., 2020; Maragno et al., 2020; Toloo et al., 2014).

Moreover, the elevated temperatures during hot spells can intensify the occurrence of cardiovascular and respiratory issues (Guo et al., 2017). Individuals with heart and lung conditions may experience heightened symptoms, and the strain on the cardiovascular system can contribute to an increased risk of heart attacks and respiratory distress (Arsad et al., 2022; Guo et al., 2017).

The indirect impacts of extreme heat on mortality are further compounded by the heightened risk of wildfires (Rossiello and Szema, 2019). As vegetation becomes dry and more prone to ignition, wildfires can rapidly spread, posing immediate threats to lives and communities (Rossiello and Szema, 2019; Sander, 2022). The inhalation of smoke and particulate matter from wildfires can exacerbate respiratory conditions, potentially leading to respiratory failure and increased mortality rates, particularly among vulnerable individuals (Rossiello and Szema, 2019).

The UK Health Security Agency's Heat Mortality Monitoring Report for 2022 reveals a notable impact on heat-related deaths during the summer of 2022, specifically across five distinct episodes (UKHSA, 2023). Among these episodes, two did not exhibit any significant excess deaths. In mid-June, a slight increase in all-cause deaths was observed, particularly affecting the 65 years and over group. However, the remaining two episodes witnessed a notably higher excess death rate (DEFRA, 2018; UKHSA, 2023).

In mid-July, one episode recorded 1256 excess deaths, with significant mortality observed in the 65 years and over group. Similarly, in early August, another episode saw an estimated 1633 excess deaths, with substantial excess deaths noted in both the 45 to 65 years and 65 years and over age groups (UKHSA, 2023). The findings emphasised the significant impact of heatwaves on mortality, particularly among the middle-aged and elderly demographic. These statistics underscore the urgency of mitigating extreme heat events.

### 1.2. Urban heat islands and extreme weather events

The occurrence of extreme weather events could be exacerbated by the influence of Urban Heat Island (UHI) within cities (Eugenio Pappalardo et al., 2023; Zhao et al., 2018). UHI characterises localised zones in urban environments, typically cities, where temperatures are considerably higher than those in the surrounding rural areas (Santamouris, 2020). Metropolitan areas suffer from the UHI, where the temperature difference between the city centre and the surrounding rural and suburban areas can reach several degrees Celsius. The built environment in cities, characterised by concrete, asphalt, and other heat-absorbing materials, tends to retain and radiate heat, leading to elevated temperatures (Elmarakby and Elkadi, 2024; Li et al., 2020).

In densely populated cities, the built environment often becomes compacted to accommodate the growing population at the expense of green cover and natural surfaces. The expansion of the built environment, at the cost of reducing green cover, contributes to the city's heat retention and exacerbates the UHI effect (Eugenio Pappalardo et al., 2023; Zhao et al., 2018).

While UHI has various consequences, such as increased energy demand for cooling buildings, its most perilous impact lies in exacerbating the effects of heat waves. These heat islands can have notable impacts on extreme weather events, heightening their intensity in cities and contributing to various environmental challenges (Eugenio Pappalardo et al., 2023).

During heatwaves, UHIs intensify the overall warmth, making cities more susceptible to extreme temperatures (Zhao et al., 2018). This augmented temperature can pose severe health risks to urban populations, especially vulnerable groups such as older people and those with pre-existing health conditions (Dong et al., 2020; Maragno et al., 2020; Zhao et al., 2018).

Urban heat islands can also interact with air pollution, creating a feedback loop that further worsens air quality during extreme weather events (Wang et al., 2a021). High temperatures can enhance the formation of ground-level ozone, exacerbating respiratory problems and negatively impacting public health (Ulpiani, 2021; Wang et al., 2021).

Mitigating the impact of urban heat islands involves implementing strategies such as increasing green spaces, incorporating reflective surfaces, and designing energy-efficient buildings (Elmarakby et al., 2020; Zhao et al., 2018). These measures not only help cool urban environments but also contribute to overall resilience against the adverse effects of climate change (Fadhil et al., 2023). Addressing the UHI effect is crucial for building sustainable and climate-resilient cities.

### 1.3. Green infrastructure for mitigating urban heat islands effect

Green infrastructure is one of the comprehensive and strategic approaches to combat the UHI effect and counter the impacts of extreme heat waves in cities (Leal Filho et al., 2021; Marando et al., 2022). Unlike conventional grey infrastructure that relies on manufactured materials, green infrastructure harnesses living systems and natural processes to provide various environmental benefits (Aram et al., 2019). Within the urban landscape, green infrastructure incorporates verdant spaces and planting open spaces and roads as integral components of the city's infrastructure (Aram et al., 2019; Leal Filho et al., 2021). This strategic approach fosters cooler environments that not only mitigate the UHI impact but also provide additional benefits, such as contributing to biodiversity, offering recreational spaces, and enhancing the city's aesthetic appeal (Aram et al., 2019; Zhou et al., 2023).

Green infrastructure extends to buildings, incorporating features like Green Roofs and Walls that enhance insulation, reduce energy consumption, and mitigate the UHI effect (Balany et al., 2020). In addition, utilising permeable pavements and surfaces within green infrastructure reduces heat retention compared to asphalt. These surfaces also contribute to sustainable water management, allowing water to infiltrate the ground, mitigating runoff, and supporting groundwater recharge (Balany et al., 2020). Moreover, studies have underscored the critical role of blue-green spaces in alleviating the adverse effects of climate change in urban environments. Blue-green spaces, such as parks, gardens, and water bodies, offer substantial cooling effects by reducing surface and air temperatures through evapotranspiration and shading mechanisms. The (2020) study by Yu et al. has shown that urban vegetation significantly contributes to cooling urban environments through mechanisms such as evapotranspiration and shading, particularly during extreme heat waves (Yu et al., 2020). This process aids in cooling the urban environment, contributing to temperature regulation and reducing the UHI effect in cities (Aram et al., 2019; Yu et al., 2020).

Therefore, integrating green infrastructure into urban planning emerges as a multifaceted and effective strategy, fostering natural cooling, improving air quality, and enhancing overall urban resilience, thereby creating sustainable and comfortable urban environments. The systematic deployment of green infrastructure not only contributes to reducing ambient temperatures but also fosters healthier and more sustainable urban environments. High-risk zones can gain prioritised attention by strategically integrating vegetation, green roofs, and other green infrastructure solutions to bolster their resilience against UHI effects.

While many UHI mitigation strategies focus on individual landscapes or certain contexts and locations, recent studies have emphasised the importance of identifying key UHI nodes and links from a connectivity and network perspective at a regional scale to target high-risk areas effectively (Yu et al., 2024).

Implementation of UHI mitigation interventions, whether green infrastructure or other strategies, necessitates prioritisation. Addressing areas with the most urgent needs before others is essential, as this approach ensures efficiency and optimal resource allocation. Consequently, identifying areas of high heat-risk vulnerability becomes imperative for prioritising interventions effectively. Developing risk maps is crucial to facilitate this prioritisation process, as they identify zones requiring immediate UHI mitigation strategies.

Heat Risk maps should serve as a smart tool in this process, offering a visual representation of areas most susceptible to UHI and aiding urban planners and policymakers in making informed decisions on resource allocation for UHI mitigation strategies, including green interventions. Thus, this study aims to guide a smart implementation of UHI mitigation strategies by developing and testing a heat risk index that visually maps the areas needing immediate intervention to mitigate the UHI. Using Manchester City as a case study, this paper relies on three variables to build the risk index: the spatial intensity of Urban Heat Islands (UHIs), current green cover, and population density.

This heat risk index serves as a prioritisation tool to roughly identify areas requiring immediate green infrastructure interventions for mitigating UHI based on heightened population, lack of green cover, and intensified UHI impact. Applying the heat risk index guides urban planners and decision-makers in focusing their efforts to enhance cities' resilience against the rising threat of extreme heat and UHI.

This paper is structured into four sections. The first part, the literature review, examines existing research elucidating the correlation between extreme heat and Urban Heat Islands (UHIs), particularly emphasising enhancing urban resilience by implementing green infrastructure. Utilising Manchester City as a case study for applying the developed heat risk index, the second section, the case study and methodology, provides a detailed exploration of the formulation and testing of the index, along with the criteria for developing the HRI maps. The third section presents the paper's results and discussion, highlighting key findings and elucidating the outcomes derived from the implemented heat risk index. In the final section, the conclusion and recommendation, the paper summarises pivotal insights and furnishes recommendations for future research and practical applications based on the outcomes.

## 2. Case study and research methodology

Manchester's urban environment mirrors challenges prevalent in contemporary cities worldwide (McNeal, 2022). The city grapples with issues like high population density, ongoing infrastructure development, socioeconomic disparities, and environmental challenges (Breezometer, 2023; McNeal, 2022). Its historical significance as the first industrial city in the world, combined with current urban regeneration initiatives, positions it as a microcosm of intricate urban challenges experienced globally (Breezometer, 2023; McNeal, 2022).

Based on the Green Spaces Rating Map conducted by Friends of the Earth International (FOEI) (2020), an analysis of Manchester's districts reveals a diverse landscape in terms of access to green spaces. Out of the total districts surveyed in Manchester, twenty-five were rated as E, indicating a significant deficiency in green spaces, while twenty districts received a D rating, suggesting limited access. Additionally, six districts were classified as C, indicating moderate access, and another six as B, implying relatively better access to greenery.

Notably, none of the districts attained an A rating, indicating the absence of areas with extensive green space accessibility. The map shows a notable scarcity of green spaces that characterise the *E*-rated neighbourhoods, and as it goes toward A, districts enjoy comparatively abundant access to natural surroundings (Fig. 1) (Friends of the Earth, 2020).

This situation renders Manchester an ideal study area for assessing and applying the heat risk index, providing valuable insights into mapping districts needing urgent interventions mitigating the UHI impact to manage the extreme heat events in urban contexts.

### 2.1. Developing the risk index: Variables included

The research methodology encompasses three critical layers of data collection: Green Cover Mapping, Land Surface Temperature (LST) Calculation, and Population Data Integration, all contributing to the generation of the Heat Risk Index (HRI) for Manchester (Fig. 2). The SPSS was utilised later to test the validity of the HRI in terms of studying the correlations between the variables themselves and the variables against the HRI.

#### 2.1.1. Variable I: Population density

Higher population density means more people living and working in close proximity to urban areas. When UHIs elevate temperatures, residents are exposed to prolonged periods of heat, increasing the risk of heat-related illnesses and heat stress. Vulnerable populations, such as the elderly, children, and individuals with pre-existing health conditions, are particularly susceptible to these risks (Li et al., 2020).

In addition, high-population areas often have limited access to cooling amenities such as green spaces, parks, and trees. These natural elements help mitigate heat by providing shade and evaporative cooling. However, in densely populated areas, space for such amenities may be limited or nonexistent, reducing opportunities for residents to seek relief from the heat (Elmarakby et al., 2022).

Furthermore, during periods of extreme heat, residents in populated urban areas suffer from prolonged exposure to heat, increasing the likelihood of heat-related death and many other health issues (Dong et al., 2020).

Therefore, the study took into account population density as one of the main variables in developing the HRI.

Utilising the Office for National Statistics (ONS) data for the year 2021, the research acquired the boundaries of Manchester City, encompassing its various districts, along with the associated population figures for each district (ONS, 2021). This data was obtained as a shape file and then imported into GIS Pro. This layer facilitated the spatial representation of Manchester City's geographical boundaries, districts, and corresponding population distribution. According to the Manchester City Council and the Office for National Statistics (ONS), the most recent census data available for Manchester is from 2021, which is conducted every ten years (Manchester City Council, 2021; ONS, 2021). Therefore, this research utilised the UK 2021 population density data as the most recent population density map as an input for the Heat Risk Index (HRI).

This comprehensive dataset was the first piece in formulating and implementing the Heat Risk Index, enhancing the research's ability to assess and address urban heat-related challenges in each city district, considering the population factor.

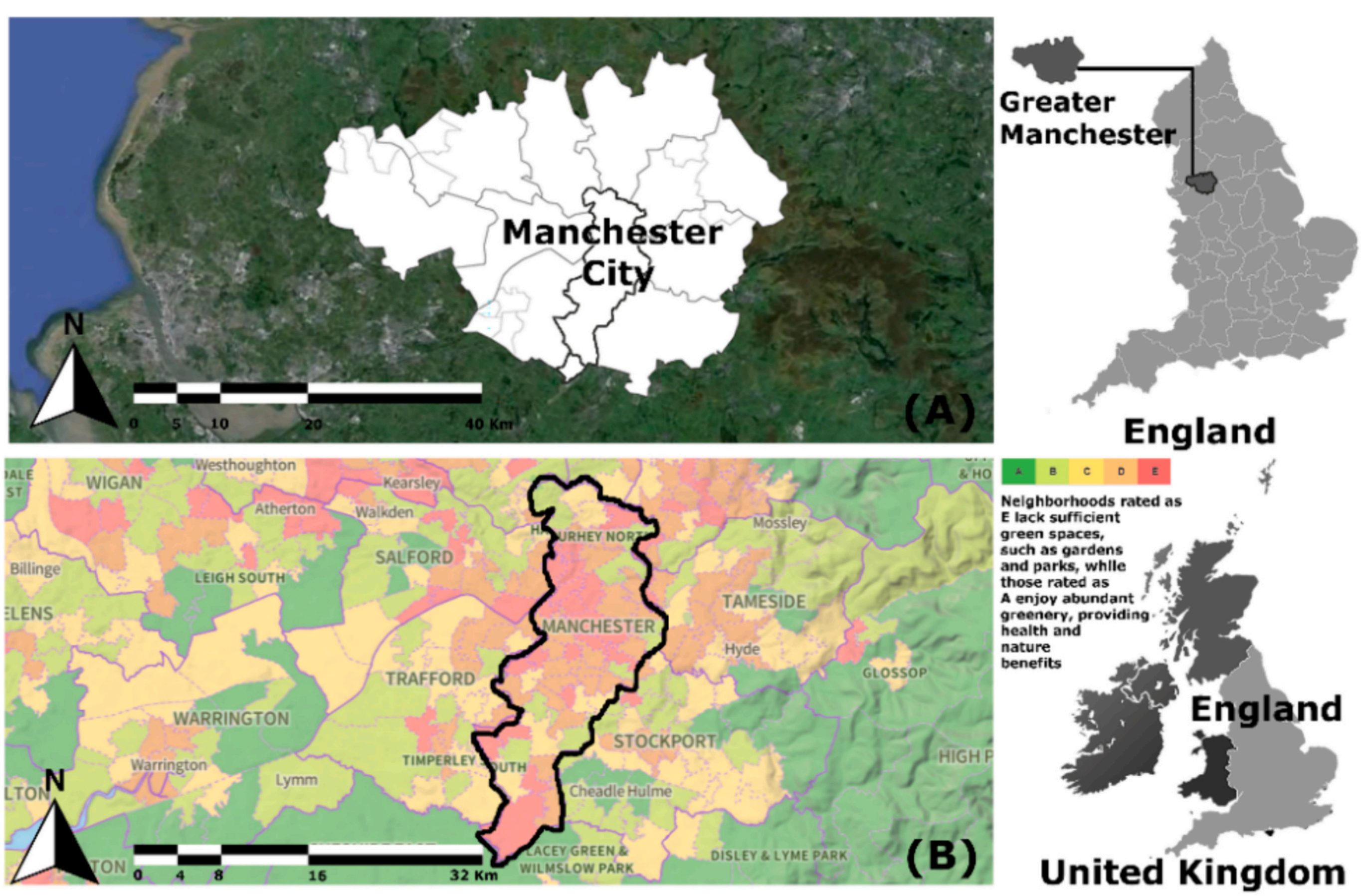


**Fig. 1.** (A) The Case Study: Manchester City; (B) Green Spaces Rating Map in Manchester based on (Friends of the Earth, 2020).


**Fig. 2.** The Research Methodology.

#### 2.1.2. *Variable II: Green cover*

High-density urban areas often have limited green spaces like parks, trees, and gardens. Green spaces provide natural cooling through shade and evapotranspiration, but in densely populated areas, these spaces are reduced, leading to less cooling effect and exacerbating the urban heat island effect (Aram et al., 2019; Elmarakby et al., 2022; Elshater et al., 2022). Thus, this study involved the green cover variable in the HRI formulation due to its importance in reducing UHI impact.

To identify green cover within the study area, the research utilised the European Space Agency WorldCover (2021) Global land cover product. This comprehensive map, collaboratively developed by the WorldCover Consortium and the European Space Agency for 2020, provides a global overview at a 10-m resolution using Sentinel-1 and 2 data, encompassing 11 generic classes describing the land surface cover (ESA, 2021).

The decision to rely on the European Space Agency's WorldCover maps was driven by the exceptionally high resolution these maps offer. With a spatial resolution of 10 m, the WorldCover maps provide a detailed and precise representation of land cover, which is crucial for accurately assessing and mapping urban heat islands. This fine level of detail allows for a more accurate analysis of urban environments, ensuring that even small patches of green cover or highly built-up areas are correctly identified. Consequently, this enhances the Heat Risk Index's overall reliability and accuracy, enabling pinpointing areas with the highest vulnerability to the Urban Heat Island effect with greater precision.

Following the extraction of the Manchester City boundary of the world map, the layer underwent raster remapping to extract green cover exclusively, including "Tree cover," "Shrubland," "Grassland," and "Cropland." This process involved assigning a value of "1" to cells representing green cover and "0" to all other cells, resulting in a focused representation of the study area's vegetative landscape. Then, the study employed the GIS tool "Zonal Statistics As Table" to generate a table detailing the count of green cover cells within each district polygon. Subsequently, two fields were added to the layer, capturing the count of green cover cells within each district and the percentage of this green cover relative to the total number of cells within each district. This approach enabled the research to assign a percentage to each district, indicating the areas lacking green cover by subtracting the percentage of green cover from 100 within each district polygon. This method facilitates a thorough examination of areas within each district that are deficient in adequate green cover.

#### 2.1.3. Variable III: Urban heat island

Considering the UHI as the base of the developed HRI formulated in this study, it was imperative to calculate and map the UHI in the study area. Remote sensing emerges as an efficient and cost-effective method for calculating the UHI(Diem et al., 2023; Tomlinson et al., 2011).

The study utilised EarthExplorer to obtain satellite images necessary for calculating Land Surface Temperature (LST). Specifically, Landsat 8–9 OLI/TIRS Collection 2 Level-2 and Landsat 8–9 OLI/TIRS Collection 2 Level-1 images were selected to analyse LST and the Urban Heat Island (UHI) effect in Manchester City (Table 1). (Kasniza Jumari et al., 2023; NASA, 2024).

EarthExplorer is a user-friendly and free platform developed by the United States Geological Survey (USGS) to obtain satellite images necessary for calculating Land Surface Temperature (LST). EarthExplorer was chosen for several key reasons. Firstly, it provides access to an extensive archive of high-quality satellite imagery, which is essential for conducting comprehensive temporal and spatial analyses (Hulley et al., 2019; Saleh, 2011). The platform's robust tools for searching, filtering, and downloading data allow researchers to efficiently locate and acquire the specific images needed for their study (Kasniza Jumari et al., 2023; NASA, 2024). Additionally, EarthExplorer supports various data formats compatible with Geographic Information Systems (GIS) and provides detailed metadata, enhancing the precision and reliability of the analysis process.

The satellite images were acquired on April 6, 2023, a typical working day, strategically chosen to represent the normal pattern of the UHI effect during weekdays. This date falls in the spring season, a deliberate choice to avoid the extreme temperatures of summer and the less pronounced UHI effects during winter. Furthermore, autumn was avoided due to the high cloud cover usually present, which can obscure satellite imagery.

To ensure the reliability of the analysis, a stringent filtering process was applied to the selected satellite images. This involved setting a cloud coverage threshold of <20 % within the designated Worldwide Reference System (WRS) scene. This criterion was crucial to achieving optimal image clarity and minimising potential interference from cloud cover and extreme weather conditions, thereby enhancing the accuracy of the LST and UHI analysis. The robustness of this filtering process is supported by previous studies (Lin et al., 2018; Weng and Fu, 2014), ensuring that the data used for analysis were of high quality.

This careful consideration of the timing and quality of satellite images aimed to provide a comprehensive and accurate assessment of the land surface temperature and UHI effects in the study area.

The thermal infrared bands (TIRS) of Landsat 8 and 9 initially capture data at a spatial resolution of 100 m, where each pixel represents an area of 100 by 100 m on the ground (USGS, 2020). However, to align with the 30-m resolution of the multispectral bands (Bands 1–7 and 9), the thermal bands (Band 10 and 11) are resampled to match this finer resolution in the standard data products (USGS, 2015, 2022). This resampling process interpolates the original 100-m data to create a more detailed grid of 30-m pixels, facilitating seamless integration and analysis with other Landsat data layers (USGS, 2020, 2022).

**Table 1**
the satellite image metadata.

| Satellite Image | Metadata |
|---|---|
| Satellite type | Landsat 8/9 |
| Sensor | OIL_TIRS |
| Path/Row | 203/023 |
| Spatial Resolution | 30 |
| Acquisition Date | Thursday 06.04.2023 |
| Acquisition Time (Z)* | 11:10:25 |
| Acquisition Time (BST)* | 12:10:25 |
| Cloud Cover | 15.17 |

* Z: Zulu time, referred to the Universal Coordinated Time (UCT), is typically converted to British Summer Local Time (BST).

For regional-scale analysis, such as mapping UHI at Manchester City (macro-scale), the impact of this resolution change may be minimal. The broader patterns of UHI intensity and spatial distribution, which are typically analysed at larger scales, can still be effectively captured and studied using resampled Landsat thermal data at a 30-m resolution (Diem et al., 2023; Kustas and Anderson, 2009). This allows for meaningful comparisons and insights into UHI dynamics across different urban settings, including Manchester, without significant compromise in study outcomes (Luo et al., 2019; Tomlinson et al., 2011).

This alignment enables comparing thermal information, such as land surface temperature, with other local resolution data set accuracies, such as population density and green cover, proving the enhanced depth of spatial analysis (Diem et al., 2023; Kustas and Anderson, 2009).

The analysis process, conducted using ArcGIS Pro, commenced with two levels of data processing, ultimately calculating land surface temperature and assessing the Urban Heat Islands based on the Landsat 9 Data Users Handbook (USGS, 2022).

In the context of the LST Calculation, the initial step involved the conversion of Digital Numbers (DN) to Spectral Radiance of the selected Band (band 10). This conversion process was executed utilising the following equation:

$$\mathrm{TOA\ (L)} = \mathrm{ML}^{*}\ \mathrm{Qcal} + \mathrm{AL} \tag{1}$$

Where TOA (L) is the Top of Atmospheric spectral radiance from the metadata, ML is the radiance multiplicative scaling factor from the metadata, Qcal is band 10, and AL is the radiance additive scaling factor.

Then, the sensor brightness temperature (BT) was calculated in degrees Celsius using the following formula:

$$\mathrm{BT\ (C)} = (\mathrm{K2}/(\mathit{ln}\ (\mathrm{K1}/\mathrm{L}) + 1\,)\,) - 273.15 \tag{2}$$

K1 and K2 are the Band-specific thermal conversion constants obtained from the metadata attached to the Landsat image, and L is the spectral radiance (TOA).

Then, the Red and Near Infra Red (NIR) bands (bands 4 and 5) were used to calculate the Normalised Difference Vegetation Index (NDVI) using the equation:

$$\mathrm{NDVI} = (\mathrm{Band\ 5–Band\ 4})/(\mathrm{Band\ 5} + \mathrm{Band\ 4}) \tag{3}$$

Calculating the Normalised difference vegetation index (NDVI) is essential for obtaining the Proportion of the Vegetation (PV) and the Emissivity as follows, which is critical to calculating LSt:

$$\mathrm{Pv} = \mathrm{Square}\ ((\mathrm{NDVI–NDVImin})/(\mathrm{NDVImax–NDVImin})\,) \tag{4}$$

$$\varepsilon = 0.004{*}\mathrm{Pv} + 0.986 \tag{5}$$

Finally, LST is calculated using the following equation:

$$\mathrm{LST} = (\mathrm{BT}/(1 + (\lambda^{*}\ \mathrm{BT}/\rho)^{*}\ \mathrm{Ln}(\varepsilon)\,)\,) \tag{6}$$

LST is the Land Surface Temperature (°C) corrected by the Emissivity ($\varepsilon$). BT is the Brightness Temperature. $\rho$=h*c/r (1.438*10–2 m K), r = Boltzmann constant (1.38*10–23 J/K), h = Planck's constant (6.626*10–34 J s), c = velocity of light (2.998 *108 m/s).

The UHI is calculated as the spectral areas with a temperature of 0.5 or more standard deviations above the mean temperature. Where μ is the mean LST, and σ is the standard deviation).

$$\mathrm{UHI} \geq \mu + 0.5\sigma \tag{7}$$

### 2.2. Heat risk index: Testing and validating

Once the input variables, including population density, UHI spatial intensity, and existing green cover, were prepared, they were amalgamated to formulate the Heat Risk Index (HRI). The criteria for selecting these variables are based on their significant impact on urban heat and public health.

- Population Density: Population density was selected because areas with higher populations are likely to have more vulnerable people exposed to heat risks, as discussed in Section 2.1.1
- Green Cover: The green cover was included as it provides cooling effects through shading and evapotranspiration, thereby mitigating the UHI effect. (see Section 2.1.2)
- UHI Spatial Intensity: was calculated from the LST to represent the hotspots within the city, highlighting areas with heightened temperature and less resilience to heat waves (Section 2.1.3).

These variables were selected due to their well-mutual influence on escalating heat stress in the cities, making them critical components for assessing heat risk in urban areas.

Before amalgamating the variables to create the heat risk index in GIS, their data values were standardised in different units of measurement. The "Standardize Field" geoprocessing tool in GIS was employed for this purpose, using the minimum-maximum standardisation method. This procedure created a 5-point scale, where "1" denoted areas with the lowest values of the variable, and "5" represented areas with the highest values of the variables. The outcome was three layers: Areas Lacking Green Cover, Population Density, and Urban Heat Islands (UHI). The values for each layer ranged from 1 to 5, scaled proportionally compared to their initial values.

Upon completion of the standardisation process, the three input variables were combined to generate the HRI for Manchester. Each variable was given equal weighting in the final index, reflecting the balanced impact of urban heat islands, green cover, and population density on heat risk.

In the amalgamated HRI, a scale ranging from 1 to 15 represents areas with the lowest to highest heat risk index in Manchester. Each variable contributes equally to the risk index: 5 points for population density, 5 points for lack of green cover, and 5 points for Urban Heat Islands. These three components are combined to create the 15-point risk index.

The rationale for equally weighting population density, UHI spatial intensity, and green cover in the selection criteria requires further justification due to their critical roles in influencing urban heat dynamics and vulnerability. Population density serves as a proxy for urban activity and infrastructure density, directly impacting heat generation and UHI intensity. UHI spatial intensity directly correlates with land surface temperature variations across urban areas, indicating areas of heightened heat accumulation and potential heat stress risks. Green cover, on the other hand, provides cooling effects through shading and evapotranspiration, mitigating UHI effects and reducing local temperatures.

Equal weighting of these variables implies that each factor contributes similarly to the overall assessment of heat risk. Justification for this approach lies in their collective impact on urban heat vulnerability, aiming for a balanced consideration of both human and environmental factors.

Subsequently, the visual representation of the HRI for Manchester was achieved by adjusting the symbology to reflect the standardised scale. This process involved employing an Arcade expression, a lightweight language within ArcGIS, to tailor the symbology and effectively visualise the HRI for Manchester.

To validate the HRI, a correlation analysis using SPSS was employed to examine the relationships between the variables themselves and the HRI. This approach was adopted to assess the effectiveness of the HRI in accurately representing areas with the highest and lowest hazards. The correlation analysis aimed to provide insights into how well the HRI responds to the identified variables, thus validating its efficiency in portraying areas with varying levels of hazards.

In addition, correlational analysis was conducted to understand the association between the variables and how they act according to each other. The Pearson correlation coefficient analysis involved calculating correlation coefficients to quantify the strength and direction of relationships between pairs of variables. Positive correlations indicated that as one variable increased, the other also tended to increase, while negative correlations suggested an inverse relationship. Additionally, correlation coefficients close to 1 or − 1 indicated strong associations, whereas coefficients closer to 0 implied weaker correlations. This approach helps evaluate the performance of the HRI and offers any recommendations that could improve its performance.

## 3. Results and discussion

Analysis of population density distribution in Manchester reveals a pattern typical of metropolitan areas, characterised by an intensification of population density in proximity to city centres. This trend is particularly evident in areas such as Levenshulme, Moss Side, Hulme, Rusholme, Woodhouse Park, and Higher Blackley, where population density ranges from 5001 to over 10,000 residents per square kilometre (Fig. 3). Moving away from the city centre toward both the south and the north, population density gradually decreases to an average of 500–1500 residents per square kilometre (Fig. 3).

In addition, the high population density observed in Manchester corresponds to a more condensed urban structure and a notable lack of green cover in densely populated areas. The mapping analysis highlights that green cover is more prevalent in less populated regions toward the north and south of Manchester. Conversely, areas in and around the city centre exhibit a conspicuous absence of green cover, attributable to the higher population density and the prevalent compact urban layout in these areas.

Furthermore, the remote sensing analysis allowed the paper to calculate the Land Surface Temperature (LST), which was used as the baseline for mapping the UHI. The UHI intensity map in Manchester revealed that around 29.21 % of Manchester City is impacted by UHI (Fig. 3), where heat pockets within the city's urban structure exceeded three degrees Celsius. Hotspots of heat concentration are prominently clustered around the city centre, aligning with the observed scarcity of green cover and the heightened population density. Conversely, these hotspots diminish in frequency toward the northern and southern regions of the city.

Comparing the UHI map and the land cover to population density maps showed that the increase in LST and the decrease in green cover are closely linked to higher population density. This surge in population density stimulates the expansion of built-up areas, accommodating the increased population and leading to a notable decrease in green cover within these areas. These built-up areas exhibit surfaces with impermeable properties, such as concrete and asphalt, allowing them to store and trap heat, contributing to the elevation of LST and the formation of heat islands associated with the spread of the built-up areas. These results indicate that areas with higher green cover exhibit lower temperatures, supporting previous findings on the cooling benefits of urban vegetation (Yu et al., 2020).

The results in this study line up with another study conducted in (2010), a collaborative effort involving the Royal Meteorological Society, Reading, the University of Manchester, and Altrincham Grammar School for Girls, Cheshire. It revealed significant temperature disparities across Greater Manchester, with central Manchester experiencing the highest temperatures and areas south of Trafford recording the lowest temperatures, resulting in a notable difference of almost three °C between the warmest and coolest areas (Knight et al., 2010). Further analysis of temperature variations across different land use types

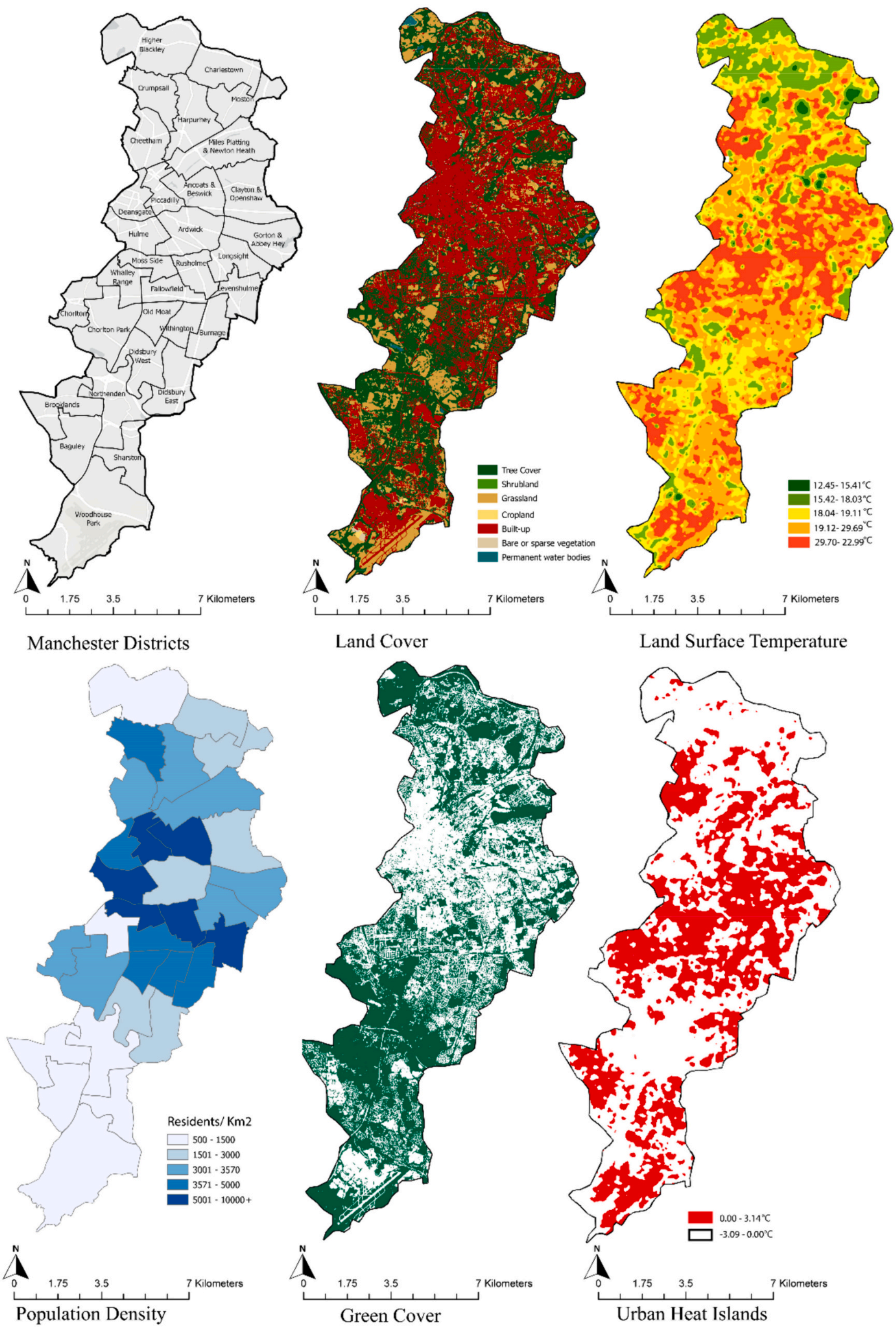


**Fig. 3.** Mapping the HRI's three variables: population density, Green Cover, and the Urban Heat Islands.

unveiled that areas characterised by high building density and limited vegetative surface cover tended to exhibit comparatively higher temperatures that can reach up to approximately 3 °C during the day, escalating to 5 °C at night (Knight et al., 2010). This experiment, conducted by a multidisciplinary team, provided a snapshot of spatial temperature patterns during a period expected to showcase urban-rural thermal contrasts, highlighting extreme conditions rather than typical averages. These results align with the UHI mapping in this paper (Fig. 3), which shows that Manchester's urban heat island (UHI) effect reaches up to approximately 3 °C.

Overlapping the three variables: population density, green cover, and the UHI, the Heat Risk Index (HRI) was developed. Each variable was taken a score out of 5, rending the total score of the HRI out of 15 where areas at great risk exposed values over 10 out of 15 on the scale, such as Moss Side, Ancoats, Beswick, Piccadilly, Hulme, Rusholme, Cheetham, Ardwick, and Withington (Fig. 4). These areas are vulnerable to heat hotspots due to a lack of green cover and high population density, posing significant health risks to residents. Other disparities were noticed between Manchester districts, where districts in the north and south exhibited less risk. These results align with the Manchester City Council Report (2022) for information on the impact of the recent heatwave, highlighting concerns about physical and mental health and resilience building across Manchester. Climate projections in the study indicated that Manchester would experience warmer summers in the future, with an increased likelihood of very intense heatwaves. This is particularly problematic in the city centre, where buildings, especially high-rise apartments, retain heat overnight. This can lead to increased heat and air quality risks, particularly affecting residents in Manchester's city centre and high-density urban areas, thereby elevating their risk of health-related illnesses (Manchester City Council, 2022).

The HRI demonstrated a strong alignment with the three variables: population density, green cover, and UHI. High-risk districts were observed to be concentrated toward the city centre, characterised by high population density, a lack of green cover, and elevated UHI levels. These identified high-risk areas represent a high priority for interventions, emphasising implementing UHI mitigation strategies and green infrastructure to mitigate UHI effects effectively.

Conversely, low-risk areas were observed in districts located toward the north and south of the city, featuring lower population density, higher green cover, and lower UHI. Low-risk districts to the north included districts such as Harpurhey, Charlestown, and Higher Blackley, while those to the south encompassed Northenden, Sharston, and Baguley.

The HRI mapped in this paper showed a significant alignment with the urban heat risk map developed for Manchester in (2023), a collaborative effort involving the Met Office, Manchester City Council, and the Manchester Climate Change Agency to map heat vulnerability within the city (Met Office et al., 2023). The urban heat risk map showed that urban area vulnerability was associated with high urban density and population concentration toward the city centre, which tends to display heightened vulnerability to heat in Manchester (Met Office et al., 2023). This urban heat risk map focused on mapping heat vulnerability by considering variables such as population characteristics and areas experiencing more frequent heat days over 25 °C. The significant UHI impact in Manchester underscores the critical need for climate change adaptation strategies in urban planning. Integrating green infrastructure, such as parks, green roofs, and street trees, to mitigate the UHI effect by lowering surface temperatures and improving air quality. Additionally, designing buildings with heat-resistant materials and improved ventilation can reduce heat retention (Yu et al., 2020). These measures address the immediate impacts of heatwaves and poor air quality augmented by UHI and enhance the city's long-term resilience to climate change.

The Heat Risk Index (HRI) findings that were explored in this study exhibit alignment and divergence from Manchester's (2023) urban heat risk map. The urban heat risk map highlighted factors such as high urban density and population concentration near the city centre, contributing significantly to heat vulnerability (Met Office et al., 2023). In contrast, the HRI in this study, while aligned in identifying areas of high vulnerability related to urban density and population concentration, introduces additional insights by explicitly considering the UHI effect.

The divergence arises primarily due to the HRI's explicit focus on UHI, which influences local heat patterns independently of broader climatic conditions. UHI can exacerbate temperatures in specific urban microclimates, leading to localised hotspots that broader-scale vulnerability assessments may not fully capture. Therefore, areas experiencing intense UHI effects might show higher heat risk according to the HRI but could be less prominent in the general urban heat risk map if UHI was not explicitly considered.

Additionally, conducting a comprehensive analysis to assess the correlation between variables used in the index is crucial; without it, the reliability of the scale may be compromised.

Thus, while both the HRI and the 2023 urban heat risk map of Manchester identify high-vulnerability areas related to urban density and population concentration, the HRI provides a more nuanced understanding by incorporating UHI effects. The potential reasons for these differences lie in the HRI's specific focus on UHI and its methodological approach, which may capture local variations in heat risk that are not fully addressed in broader vulnerability assessments.

Therefore, this paper not only maps the Heat Risk Index (HRI) but also rigorously validates it through SPSS correlational analyses. The analysis revealed a significant positive correlation between the HRI and three critical variables: population density, lack of green cover, and the presence of urban heat islands (UHI), with significance levels consistently at 0.01 (2-tailed) (See Table 2). These findings underscore the robustness of the HRI in accurately reflecting areas with heightened risks due to increased population density and vulnerability. The analysis also highlights the crucial role of green cover in mitigating the adverse effects of UHI. By demonstrating these strong correlations, this study confirms the effectiveness of the HRI as a comprehensive tool for identifying and addressing heat vulnerability, thereby providing a solid foundation for urban planning and public health interventions aimed at reducing heat-related risks. Furthermore, all correlations among the three variables demonstrated positive associations, implying that an increase in one variable coincided with increases in the others. Notably, the correlation was most significant at the 0.01 level (2-tailed) between population density and the spread of areas lacking green cover, exhibiting $r = 0.646^{**}$; $p < 0.001$. Although the correlations between population density and UHI, as well as UHI and areas lacking green cover, were positive, they lacked statistical significance. The correlations between UHI and population density ($r = 0.154$; $p = 0.408$) and between UHI and the lack of green cover ($r = 0.061$; $p = 0.745$) were found to be not statistically significant.

Therefore, to attain higher significance correlations at 0.01 (2-tailed) across all variables and enhance the HRI's responsiveness, the paper recommends applying the HRI at a smaller scale, such as the neighbourhood level. This localised approach would offer more significant correlations between the variables and provide a more precise analysis tailored to the specific conditions of each area within the districts.

## 4. Conclusion and recommendations

This paper endeavours to apply a Heat Risk Index (HRI) in Manchester City, delineating areas with varying risk levels to Urban Heat Island (UHI) in terms of population density susceptible to UHI triggered by a lack of green cover. The analysis revealed that approximately one-third of the city is affected by UHI, with hotspots concentrated toward the city centre.

The HRI, significantly correlated with the addressed variables: population density, green cover, and UHI, highlighted high-risk areas of the districts around the city centre and low-risk zones toward the north and south. These results emphasise the importance of implementing green

| No. | Area Name | UHI | Lacking Green Cover | Density | HRI |
|---|---|---|---|---|---|
| 1 | Ardwick | 4.02 | 4.23 | 2.13 | 10.38 |
| 2 | Baguley | 3.59 | 2.09 | 1.51 | 7.19 |
| 3 | Burnage | 3.67 | 2.97 | 2.95 | 9.59 |
| 4 | Charlestown | 2.30 | 2.52 | 1.92 | 6.74 |
| 5 | Cheetham | 4.14 | 4.13 | 2.33 | 10.60 |
| 6 | Chorlton | 3.72 | 2.40 | 2.33 | 8.46 |
| 7 | Chorlton Park | 3.57 | 1.88 | 2.33 | 7.79 |
| 8 | Clayton & Openshaw | 3.45 | 3.43 | 2.13 | 9.01 |
| 9 | Crumpsall | 2.96 | 3.01 | 2.95 | 8.92 |
| 10 | Deansgate | 1.88 | 5.00 | 2.74 | 9.62 |
| 11 | Didsbury East | 3.58 | 2.60 | 1.92 | 8.10 |
| 12 | Didsbury West | 3.35 | 2.18 | 1.92 | 7.45 |
| 13 | Fallowfield | 4.19 | 2.95 | 2.95 | 10.09 |
| 14 | Gorton & Abbey Hey | 3.53 | 3.24 | 2.33 | 9.11 |
| 15 | Harpurhey | 2.73 | 2.77 | 2.33 | 7.84 |
| 16 | Higher Blackley | 2.38 | 1.90 | 1.21 | 5.49 |
| 17 | Hulme | 3.66 | 4.07 | 4.18 | 11.91 |
| 18 | Levenshulme | 3.71 | 3.38 | 3.77 | 10.86 |
| 19 | Longsight | 4.02 | 3.44 | 2.36 | 9.83 |
| 20 | Moss Side | 5.00 | 4.27 | 4.18 | 13.45 |
| 21 | Miles Platting & Newton Heath | 3.74 | 3.20 | 2.33 | 9.28 |
| 22 | Moston | 2.38 | 2.89 | 2.13 | 7.40 |
| 23 | Northenden | 3.35 | 1.69 | 1.31 | 6.35 |
| 24 | Old Moat | 3.97 | 2.89 | 2.95 | 9.80 |
| 25 | Piccadilly | 2.97 | 4.87 | 5.00 | 12.85 |
| 26 | Rusholme | 4.03 | 3.02 | 3.77 | 10.82 |
| 27 | Sharston | 3.90 | 2.17 | 1.51 | 7.58 |
| 28 | Whalley Range | 3.94 | 2.80 | 1.31 | 8.05 |
| 29 | Withington | 3.98 | 3.20 | 2.95 | 10.12 |
| 30 | Woodhouse Park | 3.63 | 2.71 | 1.10 | 7.45 |
| 31 | Ancoats & Beswick | 3.21 | 3.71 | 5.00 | 11.93 |

Mapping HRI

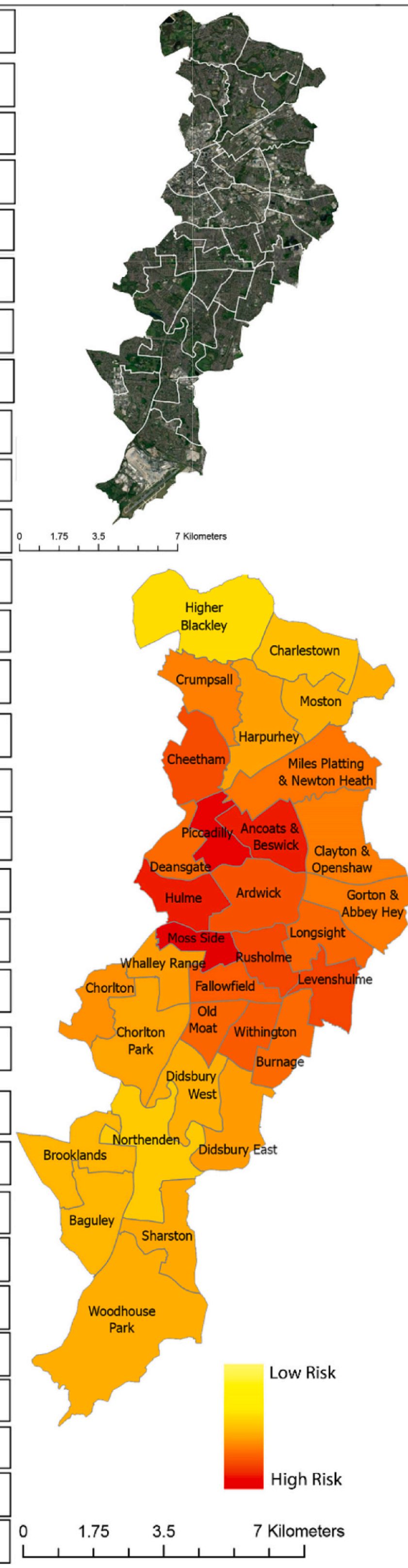


**Fig. 4.** The HRI in Manchester City's Districts.

**Table 2**
SPSS Correlation analysis: population Density, Area Lacing Green Cover, UHI, and the HRI.*

| | | Lacking Green Cover | Density | UHI | HRI |
|---|---|---|---|---|---|
| Lacking Green Cover | Pearson Correlation | 1 | 0.646** | 0.061 | 0.817** |
| | Sig. (2-tailed) | | <0.001 | 0.745 | <0.001 |
| | N | 31 | 31 | 31 | 30 |
| Density | Pearson Correlation | 0.646** | 1 | 0.154 | 0.884** |
| | Sig. (2-tailed) | <0.001 | | 0.408 | <0.001 |
| | N | 31 | 31 | 31 | 30 |
| UHI | Pearson Correlation | 0.061 | 0.154 | 1 | 0.497** |
| | Sig. (2-tailed) | 0.745 | 0.408 | | 0.005 |
| | N | 31 | 31 | 31 | 30 |
| HRI | Pearson Correlation | 0.817** | 0.884** | 0.497** | 1 |
| | Sig. (2-tailed) | <0.001 | <0.001 | 0.005 | |
| | N | 30 | 30 | 30 | 30 |

* Correlation is significant at the 0.05 level (2-tailed).
** Correlation is significant at the 0.01 level (2-tailed).

infrastructure in the identified high-risk districts around the city centre.

The paper suggests that although there was a significant correlation between the variables under consideration (population density, green cover, UHI and the Heat Risk Index (HRI), the significance of the correlation between some variables, such as UHI and green cover as well as UHI and population density, were not significantly pronounced. Therefore, it is recommended that the analysis be refined by applying the HRI at a smaller scale, such as the neighbourhood level, rather than focusing on the district scale, as used in this paper. This recommendation aims to improve the significance of the correlations between the variables. By conducting the analysis at a more localised level, mapping the HRI would be more precise and tailored to the specific conditions and characteristics of each neighbourhood within the larger district. This localised approach would enhance the accuracy and effectiveness of the analysis, providing a more detailed understanding of the factors contributing to urban heat risk.

Moreover, this Heat Risk Index serves as an initial step in creating a tool tailored for cities dealing with the challenges of Urban Heat Islands (UHI). While the existing HRI provides a foundation for assessing the level of heat hazard within a district, the suggestion is to advance and broaden its capabilities. Advanced HRI should tackle more refined and comprehensive variables that go beyond the current variables studied in this paper. Variables that could be integrated into the index should focus more on population vulnerability, specifically considering residents' medical conditions and age groups. In addition, variables related to the urban structure and the weather conditions should be taken into consideration. Finally, HRI could benefit significantly from any mapped future scenarios related to the heat pattern of the cities. By expanding the scope of variables, the refined HRI aims to improve its efficacy in capturing subtle aspects of susceptibility to extreme heat events and UHI.

However, adapting the Heat Risk Index (HRI) to different scales and for diverse urban settings requires a thoughtful approach that considers the unique characteristics of each environment. To do this effectively, several key strategies should be employed. Firstly, local calibration is essential to understand the urban planning tools that are crucial to be mapped for each context. This involves gathering and analysing area-specific data, such as land use patterns and climatic factors, to ensure the index accurately reflects the local context. For example, factors like proximity to water bodies or exposure to air pollution may play a significant role in determining heat risk in certain areas. Variables that are most relevant to the specific challenges faced by the community should be selected carefully, such as poverty, homelessness, health conditions, and age. Secondly, the weight of these variables should be considered appropriately based on each context priority. This ensures that the index reflects the relative importance of each factor in driving heat risk within the community. Additionally, the resolution of data sets should be considered. In densely populated areas, it may be necessary to scale up or zoom in and analyse heat risk at a neighbourhood level to capture variations effectively, like in the city centre of the metropolitan areas. Climate adaptation is also crucial. By incorporating climate data, such as temperature projections and predictions for future heat waves, the index can provide more relevant and useful indicators in the face of changing environmental conditions not only for the present but also based on future scenarios. Lastly, stakeholder engagement is key. By involving city planners, public health officials, and community members in the process, valuable insights can be gathered to ensure the index meets the needs of those it aims to serve. By following these strategies, the HRI can be adapted to each context, providing valuable insights and guiding targeted interventions to mitigate heat risk effectively associated with each location. Therefore, further research would focus on a forward-looking approach to creating a more sophisticated tool capable of understanding the complex dynamics associated with urban heat risks.

## 5. Limitations and further research

1. Scale of Analysis: While the district-level analysis provides valuable insights, refining the analysis to a smaller scale, such as the neighbourhood level, could offer a more granular understanding of heat risk patterns within Manchester. This approach would enhance the applicability of the Heat Risk Index (HRI) to address localised vulnerabilities effectively. However, implementing such localised indices in other cities can present both feasibility considerations and potential challenges. Different climatic and urban conditions may require tailored methodologies to accurately capture local heat risk patterns. Cities with varying levels of data availability, urban morphology, and climate characteristics might face difficulties in standardising the HRI framework. Additionally, logistical challenges such as data collection, resource allocation, and inter-agency coordination could be challenging when deploying localised HRIs in diverse urban environments.
2. Data Quality Enhancement: Despite the comprehensive use of various datasets, including population data and satellite imagery, ongoing efforts to improve data quality and incorporate real-time or high-resolution data sources are imperative. Strengthening data accuracy and completeness would bolster the reliability and effectiveness of the HRI for informing targeted interventions.
3. While resampling Landsat thermal infrared bands to 30-m resolution enhances integration and analysis for developing the Heat Risk Index (HRI), there are limitations. The original 100-m resolution may lead to some data smoothing during interpolation, potentially reducing thermal feature sharpness. Despite alignment with multispectral bands, true thermal data resolution remains at 100 m, limiting finer detail capture. Nonetheless, this resolution is suitable for the regional scale analysis of Manchester City districts. However, for micro-level analysis requiring finer detail, such as individual city blocks or small areas within districts, the limitations of the dataset may be more pronounced.
4. The research relies on the 2021 population density and green cover data, alongside the European Space Agency WorldCover (2021) Global land cover product, because either the dataset is the most recent data available or the highest resolution for both variables. However, this choice introduces a limitation as these datasets may not capture recent changes in population distribution and land cover. Future research should consider incorporating more recent versions of these datasets as appropriate to ensure the analysis remains up-to-date and reflective of current urban dynamics, thus enhancing the accuracy of the findings. Furthermore, while the landscape of Manchester has remained relatively unchanged since 2021, it is crucial to acknowledge the potential impact of any urban development or

alterations in green cover since that time, as these factors could potentially influence the HRI.

5. Variable Expansion: Expanding the HRI framework to incorporate additional variables beyond population density, green cover, and urban heat island intensity would enhance its comprehensiveness. Variables such as socio-economic status, building density, and infrastructure resilience could offer deeper insights into the multi-faceted nature of heat risk in urban environments.
6. Temporal Dynamics Integration: Integrating temporal dynamics, including seasonal variations and long-term trends, into the HRI framework would provide a more dynamic understanding of heat risk. Accounting for temporal variability due to climate change and urban development ensures the HRI remains relevant and adaptable to evolving urban contexts.
7. Validation and Policy Relevance: Further validation of the HRI using independent datasets and stakeholder engagement is crucial to ensuring its practical relevance and effectiveness in informing policy decisions. Engaging policymakers and urban planners in the validation process strengthens the HRI's utility as a planning tool for mitigating heat-related risks and fostering resilient urban environments.

## CRediT authorship contribution statement

**Esraa Elmarakby:** Writing – review & editing, Writing – original draft, Visualization, Software, Methodology, Conceptualization. **Hisham Elkadi:** Writing – review & editing, Validation, Supervision.

## Declaration of competing interest

The authors declare that they have no known competing financial interests or personal relationships that could have appeared to influence the work reported in this paper.

## Data availability

The authors do not have permission to share data.

## References


Aram, F., Higueras García, E., Solgi, E., Mansournia, S., 2019. Urban green space cooling effect in cities. Heliyon 5 (4), 1339. https://doi.org/10.1016/J.HELIYON.2019.E01339.

Arsad, F.S., Hod, R., Ahmad, N., Ismail, R., Mohamed, N., Baharom, M., Osman, Y., Radi, M.F.M., Tangang, F., 2022. The impact of heatwaves on mortality and morbidity and the associated vulnerability factors: A systematic review. Int. J. Environ. Res. Public Health 19 (23). https://doi.org/10.3390/IJERPH192316356/S1.

Balany, F., Ng, A.W.M., Muttil, N., Muthukumaran, S., Wong, M.S., 2020. Green infrastructure as an urban Heat Island mitigation strategy—a review. Water 12 (12), 3577. https://doi.org/10.3390/W12123577.

Breezometer, 2023. Check the Air Quality in Manchester, United Kingdom - BreezoMeter. https://www.breezometer.com/air-quality-map/air-quality/united-kingdom/manchester.

Calabrese, R., Dombrowski, T., Mandel, A., Pace, R.K., Zanin, L., 2024. Impacts of extreme weather events on mortgage risks and their evolution under climate change: A case study on Florida. Eur. J. Oper. Res. 314 (1), 377–392. https://doi.org/10.1016/J.EJOR.2023.11.022.

DEFRA, 2018. November 26. Department for Environment, Food & Rural Affairs- GOV.UK, Most detailed picture yet of changing climate launched. https://www.gov.uk/government/news/most-detailed-picture-yet-of-changing-climate-launched.

Diem, P.K., Nguyen, C.T., Diem, N.K., Diep, N.T.H., Thao, P.T.B., Hong, T.G., Phan, T.N., 2023. Remote sensing for urban heat island research: Progress, current issues, and perspectives. Remote Sensing Applications: Society and Environment 101081. https://doi.org/10.1016/J.RSASE.2023.101081.

Dong, J., Peng, J., He, X., Corcoran, J., Qiu, S., Wang, X., 2020. Heatwave-induced human health risk assessment in megacities based on heat stress-social vulnerability-human exposure framework. Landsc. Urban Plan. 203 https://doi.org/10.1016/J.LANDURBPLAN.2020.103907.

Elmarakby, E., Elkadi, H., 2024. Impact of urban morphology on urban Heat Island in Manchester's transit-oriented development. J. Clean. Prod. 434, 140009 https://doi.org/10.1016/J.JCLEPRO.2023.140009.

Elmarakby, E., Khalifa, M., Elshater, A., Afifi, S., 2020. Spatial morphology and urban Heat Island: comparative case studies. Architecture and Urbanism: A Smart Outlook 441–454. https://doi.org/10.1007/978-3-030-52584-2_31.

Elmarakby, E., Khalifa, M., Elshater, A., Afifi, S., 2022. Tailored methods for mapping urban heat islands in greater Cairo region. Ain Shams Eng. J. 13 (2), 101545 https://doi.org/10.1016/J.ASEJ.2021.06.030.

Elshater, A., Abusaada, H., Alfiky, A., El-Bardisy, N., Elmarakby, E., Grant, S., 2022. Workers' satisfaction Vis-à-Vis environmental and socio-morphological aspects for sustainability and decent work. Sustainability (Switzerland) 14 (3). https://doi.org/10.3390/SU14031699.

ESA, 2021. WorldCover 2021. European Space Agency. https://worldcover2021.esa.int/.

Eugenio Pappalardo, S., Zanetti, C., Todeschi, V., 2023. Mapping urban heat islands and heat-related risk during heat waves from a climate justice perspective: A case study in the municipality of Padua (Italy) for inclusive adaptation policies. Landsc. Urban Plan. 238, 104831 https://doi.org/10.1016/J.LANDURBPLAN.2023.104831.

Fadhil, M., Hamoodi, M.N., Ziboon, A.R.T., 2023. Mitigating urban heat island effects in urban environments: strategies and tools. IOP Conference Series: Earth and Environmental Science 1129 (1), 012025. https://doi.org/10.1088/1755-1315/1129/1/012025.

Friends of the Earth, 2020. Access to green space in England. https://friendsoftheearth.uk/nature/access-green-space-england-are-you-missing-out?_ga=2.124416067.853347100.1713021124-1918144580.1713021120.

Guo, Y., Gasparrini, A., Armstrong, B.G., Tawatsupa, B., Tobias, A., Lavigne, E., Coelho, De Sousa Zanotti Stagliorio, M., Pan, X., Kim, H., Hashizume, M., Honda, Y., Leon Guo, Y. L., Wu, C. F., Zanobetti, A., Schwartz, J. D., Bell, M. L., Scortichini, M., Michelozzi, P., Punnasiri, K., … Tong, S., 2017. Heat wave and mortality: A multicountry, multicommunity study. Environ. Health Perspect. 125 (8) https://doi.org/10.1289/EHP1026.

Hanlon, H.M., Bernie, D., Carigi, G., Lowe, J.A., 2021. Future changes to high impact weather in the UK. Clim. Chang. 166 (3–4) https://doi.org/10.1007/S10584-021-03100-5.

Hopke, J.E., 2020. Connecting extreme heat events to climate change: media coverage of heat waves and wildfires. Environ. Commun. 14 (4), 492–508. https://doi.org/10.1080/17524032.2019.1687537.

Hulley, G.C., Ghent, D., Göttsche, F.M., Guillevic, P.C., Mildrexler, D.J., Coll, C., 2019. Land surface temperature. Taking the Temperature of the Earth 57–127. https://doi.org/10.1016/B978-0-12-814458-9.00003-4.

Kasniza Jumari, N.A.S., Ahmed, A.N., Huang, Y.F., Ng, J.L., Koo, C.H., Chong, K.L., Sherif, M., Elshafie, A., 2023. Analysis of urban heat islands with landsat satellite images and GIS in Kuala Lumpur Metropolitan City. Heliyon 9 (8), e18424. https://doi.org/10.1016/J.HELIYON.2023.E18424.

Kendon, M., McCarthy, M., Jevrejeva, S., Matthews, A., Williams, J., Sparks, T., West, F., 2023. State of the UK climate 2022. Int. J. Climatol. 43 (S1), 1–82. https://doi.org/10.1002/JOC.8167.

Knight, S., Smith, C., Roberts, M., 2010. Mapping Manchester's urban heat island. Weather 65 (7), 188–193. https://doi.org/10.1002/WEA.542.

Kustas, W., Anderson, M., 2009. Advances in thermal infrared remote sensing for land surface modeling. Agric. For. Meteorol. 149 (12), 2071–2081. https://doi.org/10.1016/J.AGRFORMET.2009.05.016.

Leal Filho, W., Wolf, F., Castro-Díaz, R., Li, C., Ojeh, V.N., Gutiérrez, N., Nagy, G.J., Savić, S., Natenzon, C.E., Al-Amin, A.Q., Maruna, M., Bönecke, J., 2021. Addressing the urban heat islands effect: a cross-country assessment of the role of green infrastructure. Sustainability 13 (2), 753. https://doi.org/10.3390/SU13020753.

Li, Y., Schubert, S., Kropp, J.P., Rybski, D., 2020. On the influence of density and morphology on the urban Heat Island intensity. Nature Communications 2020 11:1 11 (1), 1–9. https://doi.org/10.1038/s41467-020-16461-9.

Lin, L., Xu, Y., Wang, Z., Diao, C., Dong, W., Xie, S.P., 2018. Changes in extreme rainfall over India and China attributed to regional aerosol-cloud interaction during the late 20th century rapid industrialisation. Geophys. Res. Lett. 45 (15), 7857–7865. https://doi.org/10.1029/2018GL078308.

Luo, N., Wan, T., Hao, H., Lu, Q., 2019. Fusing high-spatial-resolution remotely sensed imagery and OpenStreetMap data for land cover classification over urban areas. Remote Sensing 11 (1), 88. https://doi.org/10.3390/RS11010088.

Manchester City Council, 2021. Census results 2021 | census and population. https://www.manchester.gov.uk/info/200088/statistics_and_intelligence/7583/census_and_population.

Manchester City Council, 2022. State of the City report 2022-Manchester City Council report for information. https://www.manchester.gov.uk/info/200088/statistics_and_intelligence/8551/state_of_the_city_report.

Maragno, D., Fontana, M.D., Musco, F., 2020. Mapping heat stress vulnerability and risk assessment at the neighborhood scale to drive urban adaptation planning. Sustainability (Switzerland) 12 (3). https://doi.org/10.3390/SU12031056.

Marando, F., Heris, M.P., Zulian, G., Udías, A., Mentaschi, L., Chrysoulakis, N., Parastatidis, D., Maes, J., 2022. Urban heat island mitigation by green infrastructure in European functional urban areas. Sustain. Cities Soc. 77, 103564 https://doi.org/10.1016/J.SCS.2021.103564.

Marx, W., Haunschild, R., Bornmann, L., 2021. Heat waves: a hot topic in climate change research. Theor. Appl. Climatol. 146 (1–2), 781–800. https://doi.org/10.1007/S00704-021-03758-Y/TABLES/3.

McNeal, A., 2022. The process of urbanization and modernization that is evolving Manchester, United Kingdom. In: History, Politics, & International Studies | History 3003 - The Globe. https://doi.org/10.33015/dominican.edu/2022.HIST.3003.01.

Met Office, 2023a. UK and global extreme events – heatwaves. https://www.metoffice.gov.uk/research/climate/understanding-climate/uk-and-global-extreme-events-heatwaves.

Met Office, 2023b. Record breaking 2022 indicative of future UK climate. , July 27. https://www.metoffice.gov.uk/about-us/press-office/news/weather-and-climate/2023/record-breaking-2022-indicative-of-future-uk-climate.
Met Office, Manchester City Council, Manchester Climate Change Agency, 2023. February. Urban Heat Risk in Manchester. https://storymaps.arcgis.com/stories/05808279555f42df99aad9a1cc180257.
Mirza, M.M.Q., 2003. Climate change and extreme weather events: can developing countries adapt? Clim. Pol. 3 (3), 233–248. https://doi.org/10.3763/CPOL.2003.0330.
NASA, 2024. Unit: Urban Surface Temperatures and the Urban Heat Island Effects | MyNASAData. https://mynasadata.larc.nasa.gov/lesson-plans/unit-urban-surface-temperatures-and-urban-heat-island-effects.
ONS, 2021. Data and Analysis from Census 2021. Office for National Statistics. https://www.ons.gov.uk/.
Rossiello, M.R., Szema, A., 2019. Health effects of climate change-induced wildfires and heatwaves. Cureus 11 (5). https://doi.org/10.7759/CUREUS.4771.
Saleh, S.A.H., 2011. Air quality over Baghdad City using earth observation and Landsat thermal data. Journal of Asian Scientific Research 1 (6), 291–298.
Sander, N., 2022, July 28. Extreme Heat in the UK and Wildfires: Why we Should Expect it to Happen Again - Lemontree. The University of Reading. https://research.reading.ac.uk/lemontree/extreme-heat-in-the-uk-and-wildfires-why-we-should-expect-it-to-happen-again/.
Santamouris, M., 2020. Recent progress on urban overheating and heat island research. Integrated assessment of the energy, environmental, vulnerability and health impact. Synergies with the global climate change. In: Energy and Buildings, vol. 207. Elsevier Ltd. https://doi.org/10.1016/j.enbuild.2019.109482
Stott, P., 2016. How climate change affects extreme weather events. Science 352 (6293), 1517–1518. https://doi.org/10.1126/SCIENCE.AAF7271.
Toloo, G., Guo, Y., Turner, L., Qi, X., Aitken, P., Tong, S., 2014. Socio-demographic vulnerability to heatwave impacts in Brisbane, Australia: A time series analysis. Aust. N. Z. J. Public Health 38 (5), 430–435. https://doi.org/10.1111/1753-6405.12253.
Tomlinson, C.J., Chapman, L., Thornes, J.E., Baker, C., 2011. Remote sensing land surface temperature for meteorology and climatology: A review. Meteorol. Appl. 18 (3), 296–306. https://doi.org/10.1002/MET.287.
UKCP, 2024. UK Climate Projections (UKCP). Met Office. https://www.metoffice.gov.uk/research/approach/collaboration/ukcp.
UKHSA, 2023, July 10. *Heat mortality monitoring report: 2022 - GOV.UK*. The UK health security agency. https://www.gov.uk/government/publications/heat-mortality-monitoring-reports/heat-mortality-monitoring-report-2022.
Ulpiani, G., 2021. On the linkage between urban heat island and urban pollution island: three-decade literature review towards a conceptual framework. Sci. Total Environ. 751, 141727 https://doi.org/10.1016/J.SCITOTENV.2020.141727.
USGS, 2015. Landsat 8 Data Users Handbook.
USGS, 2020. USGS EROS Archive - Landsat Archives - Landsat 8–9 Operational Land Imager and Thermal Infrared Sensor Collection 2 Level-1 Data | US Geological Survey. https://www.usgs.gov/centers/eros/science/usgs-eros-archive-landsat-archives-landsat-8-9-operational-land-imager-and.
USGS, 2022, February 22. Landsat 9 Data Users Handbook. US Geological Survey. https://www.usgs.gov/media/files/landsat-9-data-users-handbook.
Wang, Y., Guo, Z., Han, J., 2021. The relationship between urban heat island and air pollutants and them with influencing factors in the Yangtze River Delta. China. *Ecological Indicators* 129, 107976. https://doi.org/10.1016/J.ECOLIND.2021.107976.
Weng, Q., Fu, P., 2014. Modeling annual parameters of clear-sky land surface temperature variations and evaluating the impact of cloud cover using time series of Landsat TIR data. Remote Sens. Environ. 140, 267–278. https://doi.org/10.1016/J.RSE.2013.09.002.
Yu, Z., Chen, J., Chen, J., Zhan, W., Wang, C., Ma, W., Yao, X., Zhou, S., Zhu, K., Sun, R., 2024. Enhanced observations from an optimised soil-canopy-photosynthesis and energy flux model revealed evapotranspiration-shading cooling dynamics of urban vegetation during extreme heat. Remote Sens. Environ. 305 https://doi.org/10.1016/J.RSE.2024.114098.
Yu, Z., Yang, G., Zuo, S., Jørgensen, G., Koga, M., Vejre, H., 2020. Critical review on the cooling effect of urban blue-green space: A threshold-size perspective. Urban For. Urban Green. 49, 126630 https://doi.org/10.1016/J.UFUG.2020.126630.
Zhao, L., Oppenheimer, M., Zhu, Q., Baldwin, J.W., Ebi, K.L., Bou-Zeid, E., Guan, K., Liu, X., 2018. Interactions between urban heat islands and heat waves. Environ. Res. Lett. 13 (3), 034003 https://doi.org/10.1088/1748-9326/AA9F73.
Zhou, W., Yu, W., Zhang, Z., Cao, W., Wu, T., 2023. How can urban green spaces be planned to mitigate urban heat island effect under different climatic backgrounds? A threshold-based perspective. Sci. Total Environ. 890, 164422 https://doi.org/10.1016/J.SCITOTENV.2023.164422.